HHS Public Access

Author manuscript

*J Cell Biochem*. Author manuscript; available in PMC 2018 April 02.

Published in final edited form as:

*J Cell Biochem*. 2013 June ; 114(6): 1306–1314. doi:10.1002/jcb.24470.

# ERα Regulates Lipid Metabolism in Bone Through ATGL and Perilipin

**Korinna Wend**[1], **Peter Wend**[2], **Brian G. Drew**[3], **Andrea L. Hevener**[3], **Gustavo A. Miranda-Carboni**[2], and **Susan A. Krum**[1,*]

[1]UCLA and Orthopaedic Hospital Department of Orthopaedic Surgery and the Orthopaedic Hospital Research Center, David Geffen School of Medicine at UCLA, Los Angeles, California

[2]Department of Obstetrics and Gynecology, Jonsson Comprehensive Cancer Center, David Geffen School of Medicine at UCLA, Los Angeles, California

[3]Division of Endocrinology, Diabetes and Hypertension, Department of Medicine, David Geffen School of Medicine, University of California, Los Angeles, California

## Abstract

A decrease in bone mineral density during menopause is accompanied by an increase in adipocytes in the bone marrow space. Ovariectomy also leads to accumulation of fat in the bone marrow. Herein we show increased lipid accumulation in bone marrow from estrogen receptor alpha (ERα) knockout (ERαKO) mice compared to wild-type (WT) mice or estrogen receptor beta (ERβ) knockout (ERβKO) mice. Similarly, bone marrow cells from ERαKO mice differentiated to adipocytes in culture also have increased lipid accumulation compared to cells from WT mice or ERβKO mice. Analysis of individual adipocytes shows that WT mice have fewer, but larger, lipid droplets per cell than adipocytes from ERαKO or ERβKO animals. Furthermore, higher levels of adipose triglyceride lipase (ATGL) protein in WT adipocytes correlate with increased lipolysis and fewer lipid droplets per cell and treatment with 17β-estradiol (E2) potentiates this response. In contrast, cells from ERαKO mice display higher perilipin protein levels, promoting lipogenesis. Together these results demonstrate that E2 signals via ERα to regulate lipid droplet size and total lipid accumulation in the bone marrow space in vivo.

### Keywords

ESTROGEN RECEPTOR; ESTROGEN; ADIPOCYTES; LIPID DROPLET

Adecline in 17β-estradiol (E2) levels is an important risk factor for postmenopausal osteoporosis [Sambrook and Cooper, 2006]. E2 sustains the ratio between bone-forming osteoblasts and bone-resorbing osteoclasts, through multiple mechanisms [Krum, 2011]. E2 reduces the number of osteoclasts by inhibiting osteoclastogenic cytokines and inducing

*Correspondence to: Dr. Susan A. Krum, PhD, 615 Charles E Young Dr. South, OHRC 410, Los Angeles, CA 90095. skrum@mednet.ucla.edu.

The authors declare that they have no conflicts of interest.

Additional supporting information may be found in the online version of this article.

apoptosis in osteoclasts [Krum et al., 2008]. E2 also increases osteoblast proliferation and differentiation, and prevents osteoblast apoptosis [Kameda et al., 1997; Kousteni et al., 2002]. Both hormone replacement therapy and selective estrogen receptor modulators are effective for the treatment of osteoporosis [reviewed in Wend et al., 2012].

During aging there are fewer bone-forming osteoblasts and the bone marrow is filled with increased numbers of adipocytes [Jilka et al., 1996; Justesen et al., 2002]. Developmentally, both adipocytes and osteoblasts derive from multipotent mesenchymal stem cells (MSCs) [Park et al., 1999; Pittenger et al., 1999]. E2 deficiency increases bone marrow fat differentiation, whereas E2 replacement prevents this effect in both humans [Syed et al., 2008] and rodents [Sottile et al., 2004]. Furthermore, E2 has been shown to inhibit adipogenesis from human [Zhao et al., 2011] and mouse MSCs [Dang et al., 2002; Kumar et al., 2012]. However, the E2-dependent mechanism for these effects has remained elusive.

In adipocytes, triacylglycerols (TAGs) are the main form of energy storage in lipid droplets. The lipid droplets are surrounded by a phospholipid monolayer. The most abundant lipid droplet protein is perilipin, a phosphoprotein that regulates the packing of lipids into droplets [Bickel et al., 2009; Brasaemle, 2007]. Under basal conditions perilipin inhibits lipolysis of lipid droplets; whereas during stimulation of lipolysis, perilipin promotes the catabolism of cellular fat stores through lipases [reviewed in Zimmermann et al., 2009].

Adipose triglyceride lipase (ATGL) catalyzes the first step of lipid catabolism: hydrolysis of TAG into diacylglycerol. The expression level of ATGL regulates lipid droplet size; overexpression of ATGL results in decreased lipid droplet size, whereas ATGL ablation increases the size [Smirnova et al., 2006; Miyoshi et al., 2008]. Perilipin may also regulate lipid droplet size, however, these data are contradictory [Sawada et al., 2010; Bartholomew et al., 2012].

In addition to previous studies showing lower bone mineral density in femurs of ERα knockout (ERαKO) mice [Walker and Korach, 2004], here we report that ERα-deficiency also promotes higher bone marrow lipid content. Furthermore, we show that ERα regulates ATGL and perilipin-mediated lipid metabolism and droplet size in femurs from mice and in adipocytes differentiated from bone marrow-derived MSCs in culture.

## MATERIALS AND METHODS

### REAGENTS

17β-estradiol (E2) was purchased from Sigma-Aldrich Co. ICI 182,780 was purchased from Tocris Bioscience. The following antibodies and fluorescence dyes were used: rabbit anti-perilipin and rabbit anti-ATGL antibodies (both Cell Signaling Technology, Inc.), goat anti-rabbit Alexa 594 secondary antibody (Molecular Probes, Invitrogen Co.), Hoechst 33342 and Bodipy 493/503 (both Molecular Probes, Invitrogen Co.).

### MICE

Animal work was approved by the Animal Research Committee at the University of California, Los Angeles. ERαKO and ERβKO mice were kindly provided by Dr. Pierre

Chambon [Dupont et al., 2000]. FERKO$^{AdipoQ}$ mice were kindly provided by Dr. Andrea Hevener [Hewitt et al., 2010]. FERKO$^{AdipoQ}$ mice were created by crossing ERα$^{fl/fl}$ mice with mice expressing Cre recombinase under the control of the adiponectin (AdipoQ) promoter [Eguchi et al., 2011]. Wild-type (C57BL/6) littermates were used as controls for ERαKO mice. ERα$^{fl/fl}$ mice were used as controls for FERKO$^{AdipoQ}$. Where indicated, mice were ovariectomized or sham operated at the age of 3 months. After 2 months the femurs were paraffin embedded and H&E stains were performed using standard protocols.

## OIL RED O STAINING OF FROZEN SECTIONS OF BONE

Femurs, including bone marrow, were isolated from 7-month-old mice. The femur containing the bone marrow was decalcified using DeCal Stat (Decal Chemical Corporation) for three days and then placed in 10%, 20%, and 30% sucrose successively overnight at 4°C. Femurs were then snap frozen in Tissue-Tek® OCT™ compound (Sakura Finetek) and stored at −80°C. For Oil Red O (ORO) staining the slides were air dried for 30 min and fixed in ice-cold 10% formalin for 5 min. After rinsing three times in distilled water the slides were placed in absolute propylene glycol for 5 min and stained in 0.5% ORO in propylene glycol solution for 8 min in a 60°C oven. Slides were rinsed in 85% propylene glycol solution for 5 min and then rinsed in distilled water and mounted with aqueous mounting medium (Richard-Allen Scientific). ORO stains of the lipid droplets were quantified with the Image-Pro® PLUS Software (BioImaging Solutions, Inc.).

## PRIMARY BONE MARROW CELLS

Bone marrow cells were isolated from tibias and femurs of 4-month-old female and male mice. Cells were flushed with MEM media, supplemented with 1% L-glutamine, and 1% penicillin–streptomycin and nucleated cells were counted with a hemocytometer. Total bone marrow was incubated for 5 days in MSC media (MesenCult Basal Media, Stem-Cell Technologies, Inc.), followed by differentiation and indicated treatment for 16 days. For differentiation into adipocytes, cells were switched to adipogenic induction medium (alpha MEM, 5% charcoal-dextran treated (CDT) fetal bovine serum (Omega Scientific), supplemented with 1% L-glutamine, 1% penicillin–streptomycin and 1 μM of the PPARγ agonist GW1929 (Tocris Bioscience)). Adipocyte differentiation was analyzed by ORO staining. Lipids were stained with 60% ORO solution for 10 min at room temperature. After washing and air-drying the ORO was eluted with 100% isopropanol and quantified by optical density measurement at 500 nm with a spectrophotometer (SmartSpec™ Plus, Bio-Rad Laboratories, Inc.). The lipid droplet size as relative area per lipid droplet and number of lipid droplets per cell were quantified with the Image-Pro® PLUS Software (BioImaging Solutions, Inc.).

## RNA AND QUANTITATIVE REAL-TIME PCR

Isolation of total RNA was performed using TRIzol (Life Technologies) according to the manufacturer's protocol. cDNA was constructed using the Maxima® First Strand cDNA Synthesis Kit for RT-qPCR according to the manufacturer's instructions (Fermentas, Inc.). The primer sequences used for quantitative PCR are shown in Supplemental Table I. cDNA was subjected to quantitative PCR using the Maxima® SYBR Green/ROX qPCR MasterMix (Fermentas, Inc.).

### IMMUNOFLUORESCENCE

Living cells were incubated with 10 μM Bodipy 493/503 and 2 μg/ml Hoechst 33342 in medium (alpha MEM, 5% CDT-FBS, supplemented with 1% L-glutamine, 1% penicillin–streptomycin) for 60 min in a humidified atmosphere of 95% air and 5% $CO_2$ at 37°C protected from light. After incubation, the cells were washed with PBS and fixed with 4% paraformaldehyde for 15 min at room temperature, permeabilized in 0.2% Triton X-100 and washed again with PBS and incubated for 60 min at room temperature in blocking buffer (PBS, 0.2% Tween-20, 1% normal goat serum, 1% BSA, 0.02% sodium azide). Primary antibodies were incubated overnight. Goat anti-rabbit Alexa 594 (Molecular Probes) was used as the secondary antibody and incubated for 60 min at room temperature. After washing with PBS, coverslips were mounted onto slides with aqueous mounting medium (Richard-Allen Scientific). Images were taken with a Nikon™ *ECLIPSE* microscope (Nikon Instruments, Inc.). For the relative ATGL or Perilipin stain per cell samples were quantified with the Image-Pro® PLUS Software (BioImaging Solutions, Inc.).

### FLOW CYTOMETRY ANALYSIS

The cells were treated as described in Donato et al. [2009], with minor modifications (the incubation with Bodipy 493/503 was at room temperature for 30 min in the dark). The cells were analyzed with a flow cytometer (BD LSRFortessa™ cell analyzer, BD Biosciences). The cytometer settings for the side scatter (SSC), forward scatter (FSC) and Bodipy 493/503 stain to analyze lipids in adipocytes were dependent on the analytic sensitivity of the machine. In general for SSC the scale was set above 40 to exclude cells without lipids, for FSC the scale was set above 30 to exclude background particles and for the Bodipy 493/503 stain the scale was set above $10^2$ to exclude background staining.

### STATISTICAL ANALYSIS

All experiments represent both biological and experimental triplicates. Unless otherwise stated, error bars represent mean ±1 standard deviation. Statistical analysis was performed using GraphPad Prism® (version 5) software including Student's *t*-test.

## RESULTS

### ERαKO MICE HAVE INCREASED LIPID ACCUMULATION IN THE BONE MARROW

ERαKO mice are a good model for postmenopausal osteoporosis [Krum and Brown, 2008] as they exhibit decreased cortical bone mineral density similar to menopausal women. Thus, we hypothesized that there would be adipocyte accumulation in bone marrow of ERαKO mice as observed in postmenopausal women [Rosen and Bouxsein, 2006]. To test this hypothesis, decalcified frozen femur sections of 7-month-old wild-type (WT), ERαKO, and ERβKO mice were stained with ORO to detect adipocytes. The femurs of ERαKO mice showed nearly a twofold increase in lipid accumulation in the bone marrow compared to WT femurs (Fig. 1A,B). In ERβKO femurs the number of lipid droplets in the marrow was reduced compared to ERαKO femurs, but significantly higher than WT (Fig. 1A,B).

To assess the impact of 17β-estradiol (E2) in reducing lipid formation in bone marrow, we compared H&E stained femur sections from sham-operated and ovariectomized (OVX)

mice. There were a greater number of adipocytes in the bone marrow of E2-deficient OVX mice compared with marrow from intact, E2-replete animals (Fig. 1C).

To test whether the accumulation of bone marrow-derived adipocytes was due to cell-autonomous factors, we tested adipocyte differentiation from bone marrow cells in vitro. Bone marrow cells from 4-month-old WT, ERαKO, and ERβKO mice were isolated and cultured for 16 days with or without the PPARγ agonist GW1929. Cells from both male and female mice were used, and both sexes showed the identical responses (data not shown). Undifferentiated bone marrow (maintained without a PPARγ agonist) from ERαKO mice had a significantly increased number of spontaneously differentiated adipocytes after 16 days in culture compared to WT and ERβKO, as visualized by ORO staining (Fig. 2) and Bodipy 493/503 (BODIPY) immunofluorescence (IF) (Supplemental Fig. 1). The number of spontaneously differentiated adipocytes from ERβKO mice was not different from WT (Fig. 2, Supplemental Fig. 1). Bone marrow cells from ERαKO mice differentiated with the PPARγ agonist GW1929 also showed a significant increase in the number of adipocytes, as compared to differentiated bone marrow cells from either WT or ERβKO mice (Fig. 2, Supplemental Fig. 1).

## ERα REDUCES LIPID DROPLET SIZE IN ADIPOCYTES

Following adipocyte differentiation we observed a decrease in lipid droplet size for ERαKO, compared to WT and ERβKO mice (Fig. 3A). To quantify this, lipids in adipocytes were stained with ORO, as described above, and the lipid droplet size (relative area per lipid droplet) and the number of lipid droplets per cell were measured with Image-Pro® PLUS Software (Fig. 3B,C). After differentiation to adipocytes, the size of the lipid droplets from ERαKO mice was noticeable smaller (threefold) as compared to WT and almost twofold smaller as compared to ERβKO (Fig. 3B). Furthermore, there were significantly more lipid droplets per cell for ERαKO than WT. In contrast to ERαKO, the number of lipid droplets per adipocyte was identical between ERβKO and WT (Fig. 3C).

To confirm these findings, BODIPY stained lipid droplets were analyzed by flow cytometry (Supplemental Fig. 2). We gated $BODIPY^{hi}$ labeled cells versus SSC on the *y*-axis to determine the cytoplasmic granular intensity of the lipid droplets to either an $SSC^{hi}$ or $SSC^{low}$. There were a greater number of $BODIPY^{hi}$ $SSC^{low}$ (2.5%) cells from ERαKO mice compared with WT. Again, in contrast to ERαKO, loss of ERβ failed to stimulate an increase in lipid droplets compared with WT, and thus, findings for flow cytometry recapitulated those obtained using ORO.

ERα is important in MSCs [Syed et al., 2011] and in adipocytes. In order to determine the temporal regulation of lipid droplets by ERα we compared differentiated adipocytes from total ERαKO mice [Dupont et al., 2000] with conditional knockout mice that are deficient for ERα only in adipocytes ($FERKO^{AdipoQ}$), but not earlier in differentiation (i.e., in MSCs). Wild-type mice had no difference in lipid droplet size compared to $ERα^{fl/fl}$ mice (Supplemental Fig. 3). However, the size of the lipid droplets from $FERKO^{AdipoQ}$ mice were fourfold larger than in ERαKO and more than twofold larger than in ERβKO and similar to WT (Fig. 3). Furthermore the number of lipid droplets per cell was more than twofold lower in $FERKO^{AdipoQ}$ as compared to ERαKO and similar to both WT and ERβKO. To confirm

ERα levels in vitro, RNA was obtained from differentiated adipocytes and qPCR was performed for ERα mRNA (Supplemental Fig. 4A). Whereas, ERα was undetectable in ERαKO cells, ERα is detectable in differentiated FERKO$^{AdipoQ}$, but significantly lower than in WT cells most likely due to the presence of stromal cells in the culture. Adiponectin is known to be expressed in bone marrow adipocytes and is unchanged in all the samples tested (Supplemental Fig. 4B). Cre-recombinase is highly expressed specifically in the FERKO$^{AdipoQ}$ cells differentiated with the PPARγ agonist GW1929 (Supplemental Fig. 4C). These data suggest an impact of ERα on lipid droplet size regulation in MSCs or in stromal cells, but not in later stages of adipocyte differentiation that coincide with adiponectin expression.

To further confirm the role of estrogen receptors in the regulation of lipid droplet size, the estrogen receptor antagonist ICI 182,780 was used either alone or in combination with E2 for the entire course of differentiation, and compared to untreated WT adipocytes and ERαKO adipocytes (Fig. 4A). Treatment with 10 nM E2 for 16 days led to a significant increase in the lipid droplet size (relative area per lipid droplet) compared to control (EtOH) and ICI 182,780 (10 nM) treated adipocytes, and to ERαKO adipocytes (Fig. 4B). Furthermore, ICI 182,780 antagonized the E2-induced increase in lipid droplet size (Fig. 4B). Although E2 did not alter lipid droplet numbers per cell, ICI 182,780-treated adipocytes showed an increase in lipid droplets per cell similar to that of ERαKO (Fig. 4C). In summary, these findings confirm that E2 signals via ERα to regulate lipid droplet size.

## ERα INDUCES LIPOLYSIS THROUGH ATGL AND LIPOGENESIS THROUGH PERILIPIN

ATGL is a key player in lipolysis by catalyzing the hydrolysis of stored TAG. Furthermore, ATGL is also involved in lipid size regulation [Smirnova et al., 2006; Miyoshi et al., 2008; Sawada et al., 2010; Bartholomew et al., 2012]. Therefore we tested if E2 regulates lipolysis and lipid droplet size through ATGL. Bone marrow from WT and ERαKO mice was isolated and differentiated for 16 days in vitro in the presence of vehicle (EtOH) or 10 nM E2. The cells were fixed and stained with an antibody against ATGL. ATGL was expressed in adipocytes from WT and ERαKO mice (Fig. 5A). Quantification with Image-Pro® PLUS Software (Fig. 5B) showed that ATGL protein expression was significantly increased in WT cells by E2 treatment. The basal level of ATGL in adipocytes was more than twofold lower in ERαKO adipocytes, as compared to WT cells, and E2-treatment did not alter ATGL protein expression in ERαKO cells (Fig. 5B). To determine if this effect was due to increased transcription of ATGL by ERα, *Atgl* cDNA expression levels were analyzed by quantitative PCR. *Atgl* expression was significantly reduced in ERαKO cells compared to WT (Fig. 5C) and E2-treatment significantly increased *Atgl* expression only in WT cells, but not in ERαKO (Fig. 5C). Therefore, higher levels of ATGL protein in WT adipocytes is due at least in part to increased transcription of *Atgl* by E2 activation of ERα. In summary, higher levels of the lipase ATGL correlate overall with fewer lipids in WT bone marrow adipocytes and fewer lipid droplets per cell.

Perilipin (PLIN) plays a major role in lipogenesis by regulating the function of lipases [Brasaemle, 2007; Bickel et al., 2009; Zimmermann et al., 2009]. Since it also plays a role in lipid droplet size [Sawada et al., 2010; Bartholomew et al., 2012], we tested the influence of

E2 on perilipin expression. Bone marrow-derived adipocytes from WT and ERαKO mice were stained with an antibody against perilipin (Fig. 6A). Perilipin was detected in WT and ERαKO adipocytes, and the immunofluorescence was quantified with Image-Pro® PLUS Software (Fig. 6B). The perilipin protein content was twofold higher in ERαKO cells compared to WT regardless of treatment (vehicle control (EtOH) or 10 nM E2). E2-treatment, independent of genotype, produced a twofold decrease of perilipin protein content compared to vehicle control in both WT and ERαKO cells (Fig. 6B). Interestingly, *Plin* expression was significantly lower in differentiated adipocytes from ERαKO mice compared to WT (Fig. 6C). Furthermore, E2-treatment resulted in a 4.5-fold increase of *Plin* cDNA level for WT but had no effect in KO (Fig. 6C). Therefore, these data suggest that E2 regulates PLIN protein levels post-transcriptionally. PLIN protein levels may be stabilized in ERαKO adipocytes by post-transcriptional mechanisms. In summary, levels of the lipogenesis protein PLIN correlate with higher lipid accumulation in the ERαKO bone marrow, higher number of lipid droplets per cell.

## DISCUSSION

Postmenopausal bone loss is associated with increased lipid in the bone marrow. Similarly, there are more adipocytes in the marrow of ovariectomized mice compared to sham-operated mice. Moreover, ERαKO mice also have a decreased bone mineral density and we show here for the first time that they too display an increased number of adipocytes in the marrow cavity compared to WT. Therefore, ERα plays a protective role in regulating bone marrow fat accumulation. From these data we can conclude the role of E2 signaling via ERα in the process of lipid formation in the marrow.

Osteoblasts and adipocytes differentiate from MSCs [Park et al., 1999; Pittenger et al., 1999]. In contrast to Syed et al. [2011], the in vitro studies here provide evidence for MSCs favoring adipocyte differentiation from bone marrow-derived MSCs in the absence of ERα, matching the in vivo phenotypes of ERαKO mice and postmenopausal women. The number of adipocytes was significantly increased in bone marrow from ERαKO cells after 16 days of differentiation compared to WT and ERβKO. Furthermore even in undifferentiating conditions, bone marrow cells from ERαKO showed a higher number of adipocytes, indicating an increased spontaneous rate of differentiated adipocytes. Given these data we hypothesize that ERα represses fat formation from MSCs. Our hypothesis is supported by the findings that during aging the differentiation potential favors adipogenesis over osteogenesis [Kretlow et al., 2008] and osteoporosis may be caused due to loss of progenitor cell differentiation [Carrington, 2005].

Estrogen and ERα are known to repress intra-abdominal adipose formation [D'Eon et al., 2005]. As E2 levels decline in postmenopausal women, intra-abdominal fat increases and consistently, ERαKO mice develop more white adipose tissue in the perirenal, periovarian, and mesenteric/omental regions than WT or ERβKO mice [Ohlsson et al., 2000]. Furthermore, ERαKO mice become insulin resistant and glucose intolerant with age [Heine et al., 2000; Ribas et al., 2010]. However, the role of bone marrow adipocytes on whole body metabolism is not clear. Initial studies have shown that these cells are not a metabolic source of energy during fasting [Duque, 2008], and insulin does not have a lipogenic or

differentiating effect on them [Maurin et al., 2000]. These bone marrow adipocytes are not just passive, space filling cells, as they have a negative effect on osteoblasts [Duque, 2008] and hematopoiesis [Naveiras et al., 2009].

Nascent lipid droplets from the endoplasmic reticulum membrane are small in size and grow during lipogenesis to provide neutral lipids for mobilization [reviewed in Ducharme and Bickel, 2008; Guo et al., 2009]. It is postulated that during lipolysis lipid droplets might go through fission resulting in increased surface area facilitating interaction of lipases [reviewed in Guo et al., 2009]. We show here for the first time, that ERα is involved in lipid metabolism by regulating lipid droplet size. Lipid droplets have a smaller diameter and a higher number per cell in differentiated adipocytes from ERαKO bone marrow compared to WT and ERβKO cells. Interestingly, only the complete knockout of ERα reveals changes in lipid droplet size and number. Bone marrow adipocytes from the FERKO$^{AdipoQ}$ show no difference in these parameters compared to WT, suggesting a role for ERα in lipid droplet size before the expression of adiponectin, or a role for ERα in stromal cells to regulate lipid droplet size.

In conclusion, ERα not only regulates lipid metabolism by modulating lipid droplet size through ATGL and perilipin, but also regulates lipid metabolism starting with progenitor cells, indicating a valuable target for stem cell therapies for osteoporosis.

## Supplementary Material

Refer to Web version on PubMed Central for supplementary material.

## Acknowledgments

Grant sponsor: National Institutes of Health Office of Research on Women's Health; Grant number: HD001400-08; Grant sponsor: American Federation for Aging Research; Grant sponsor: National Cancer Institute; Grant number: CA137168-01A1.

This work was supported by a K12 BIRCWH Grant from the National Institutes of Health Office of Research on Women's Health (HD001400-08) and a grant from the American Federation for Aging Research to SAK. GAM-C was supported by a K22 Grant from the National Cancer Institute (CA137168-01A1). Flow cytometry was performed at the UCLA Broad Stem Cell Research Center Flow Cytometry Core Resource.

## References

Bartholomew SR, Bell EH, Summerfield T, Newman LC, Miller EL, Patterson B, Niday ZP, Ackerman WE, Tansey JT. Distinct cellular pools of perilipin 5 point to roles in lipid trafficking. Biochim Biophys Acta. 2012; 1821:268–278. [PubMed: 22063271]

Bickel PE, Tansey JT, Welte MA. PAT proteins, an ancient family of lipid droplet proteins that regulate cellular lipid stores. Biochim Biophys Acta. 2009; 1791:419–440. [PubMed: 19375517]

Brasaemle DL. Thematic review series: Adipocyte biology. The perilipin family of structural lipid droplet proteins: Stabilization of lipid droplets and control of lipolysis. J Lipid Res. 2007; 48:2547–2559. [PubMed: 17878492]

Carrington JL. Aging bone and cartilage: Cross-cutting issues. Biochem Biophys Res Commun. 2005; 328:700–708. [PubMed: 15694404]

Dang ZC, van Bezooijen RL, Karperien M, Papapoulos SE, Lowik CW. Exposure of KS483 cells to estrogen enhances osteogenesis and inhibits adipogenesis. J Bone Miner Res. 2002; 17:394–405. [PubMed: 11878304]

D'Eon TM, Souza SC, Aronovitz M, Obin MS, Fried SK, Greenberg AS. Estrogen regulation of adiposity and fuel partitioning. Evidence of genomic and non-genomic regulation of lipogenic and oxidative pathways. J Biol Chem. 2005; 280:35983–35991. [PubMed: 16109719]

Donato MT, Martinez-Romero A, Jimenez N, Negro A, Herrera G, Castell JV, O'Connor JE, Gomez-Lechon MJ. Cytometric analysis for drug-induced steatosis in HepG2 cells. Chem Biol Interact. 2009; 181:417–423. [PubMed: 19647728]

Ducharme NA, Bickel PE. Lipid droplets in lipogenesis and lipolysis. Endocrinology. 2008; 149:942–949. [PubMed: 18202123]

Dupont S, Krust A, Gansmuller A, Dierich A, Chambon P, Mark M. Effect of single and compound knockouts of estrogen receptors alpha (ERalpha) and beta (ERbeta) on mouse reproductive phenotypes. Development. 2000; 127:4277–4291. [PubMed: 10976058]

Duque G. Bone and fat connection in aging bone. Curr Opin Rheumatol. 2008; 20:429–434. [PubMed: 18525356]

Eguchi J, Wang X, Yu S, Kershaw EE, Chiu PC, Dushay J, Estall JL, Klein U, Maratos-Flier E, Rosen ED. Transcriptional control of adipose lipid handling by IRF4. Cell Metab. 2011; 13:249–259. [PubMed: 21356515]

Guo Y, Cordes KR, Farese RV Jr, Walther TC. Lipid droplets at a glance. J Cell Sci. 2009; 122:749–752. [PubMed: 19261844]

Heine PA, Taylor JA, Iwamoto GA, Lubahn DB, Cooke PS. Increased adipose tissue in male and female estrogen receptor-alpha knockout mice. Proc Natl Acad Sci USA. 2000; 97:12729–12734. [PubMed: 11070086]

Hewitt SC, Kissling GE, Fieselman KE, Jayes FL, Gerrish KE, Korach KS. Biological and biochemical consequences of global deletion of exon 3 from the ER alpha gene. FASEB J. 2010; 24:4660–4667. [PubMed: 20667977]

Jilka RL, Weinstein RS, Takahashi K, Parfitt AM, Manolagas SC. Linkage of decreased bone mass with impaired osteoblastogenesis in a murine model of accelerated senescence. J Clin Invest. 1996; 97:1732–1740. [PubMed: 8601639]

Justesen J, Stenderup K, Eriksen EF, Kassem M. Maintenance of osteoblastic and adipocytic differentiation potential with age and osteoporosis in human marrow stromal cell cultures. Calcif Tissue Int. 2002; 71:36–44. [PubMed: 12200657]

Kameda T, Mano H, Yuasa T, Mori Y, Miyazawa K, Shiokawa M, Nakamaru Y, Hiroi E, Hiura K, Kameda A, Yang NN, Hakeda Y, Kumegawa M. Estrogen inhibits bone resorption by directly inducing apoptosis of the bone-resorbing osteoclasts. J Exp Med. 1997; 186:489–495. [PubMed: 9254647]

Kousteni S, Chen JR, Bellido T, Han L, Ali AA, O'Brien CA, Plotkin L, Fu Q, Mancino AT, Wen Y, Vertino AM, Powers CC, Stewart SA, Ebert R, Parfitt AM, Weinstein RS, Jilka RL, Manolagas SC. Reversal of bone loss in mice by nongenotropic signaling of sex steroids. Science. 2002; 298:843–846. [PubMed: 12399595]

Kretlow JD, Jin YQ, Liu W, Zhang WJ, Hong TH, Zhou G, Baggett LS, Mikos AG, Cao Y. Donor age and cell passage affects differentiation potential of murine bone marrow-derived stem cells. BMC Cell Biol. 2008; 9:60. [PubMed: 18957087]

Krum SA. Direct transcriptional targets of sex steroid hormones in bone. Journal of cellular biochemistry. 2011; 112:401–448. [PubMed: 21268060]

Krum SA, Brown M. Unraveling estrogen action in osteoporosis. Cell Cycle. 2008; 7:1348–1352. [PubMed: 18418063]

Krum SA, Miranda-Carboni GA, Hauschka PV, Carroll JS, Lane TF, Freedman LP, Brown M. Estrogen protects bone by inducing Fas ligand in osteoblasts to regulate osteoclast survival. EMBO J. 2008; 27:535–545. [PubMed: 18219273]

Kumar A, Ruan M, Clifton K, Syed F, Khosla S, Oursler MJ. TGF-beta mediates suppression of adipogenesis by estradiol through connective tissue growth factor induction. Endocrinology. 2012; 153:254–263. [PubMed: 22067314]

Maurin AC, Chavassieux PM, Frappart L, Delmas PD, Serre CM, Meunier PJ. Influence of mature adipocytes on osteoblast proliferation in human primary cocultures. Bone. 2000; 26:485–489. [PubMed: 10773588]

Miyoshi H, Perfield JW II, Obin MS, Greenberg AS. Adipose triglyceride lipase regulates basal lipolysis and lipid droplet size in adipocytes. J Cell Biochem. 2008; 105:1430–1436. [PubMed: 18980248]

Naveiras O, Nardi V, Wenzel PL, Hauschka PV, Fahey F, Daley GQ. Bone-marrow adipocytes as negative regulators of the haematopoietic microenvironment. Nature. 2009; 460:259–263. [PubMed: 19516257]

Ohlsson C, Hellberg N, Parini P, Vidal O, Bohlooly YM, Rudling M, Lindberg MK, Warner M, Angelin B, Gustafsson JA. Obesity and disturbed lipoprotein profile in estrogen receptor-alpha-deficient male mice. Biochem Biophys Res Commun. 2000; 278:640–645. [PubMed: 11095962]

Park SR, Oreffo RO, Triffitt JT. Interconversion potential of cloned human marrow adipocytes in vitro. Bone. 1999; 24:549–554. [PubMed: 10375196]

Pittenger MF, Mackay AM, Beck SC, Jaiswal RK, Douglas R, Mosca JD, Moorman MA, Simonetti DW, Craig S, Marshak DR. Multilineage potential of adult human mesenchymal stem cells. Science. 1999; 284:143–147. [PubMed: 10102814]

Ribas V, Nguyen MT, Henstridge DC, Nguyen AK, Beaven SW, Watt MJ, Hevener AL. Impaired oxidative metabolism and inflammation are associated with insulin resistance in ERalpha-deficient mice. Am J Physiol Endocrinol Metab. 2010; 298:E304–E319. [PubMed: 19920214]

Rosen CJ, Bouxsein ML. Mechanisms of disease: Is osteoporosis the obesity of bone? Nature Clinical Practice. Rheumatology. 2006; 2:35–43. [PubMed: 16932650]

Sambrook P, Cooper C. Osteoporosis. Lancet. 2006; 367:2010–2018. [PubMed: 16782492]

Sawada T, Miyoshi H, Shimada K, Suzuki A, Okamatsu-Ogura Y, Perfield JW II, Kondo T, Nagai S, Shimizu C, Yoshioka N, Greenberg AS, Kimura K, Koike T. Perilipin overexpression in white adipose tissue induces a brown fat-like phenotype. PLoS ONE. 2010; 5:e14006. [PubMed: 21103377]

Smirnova E, Goldberg EB, Makarova KS, Lin L, Brown WJ, Jackson CL. ATGL has a key role in lipid droplet/adiposome degradation in mammalian cells. EMBO Rep. 2006; 7:106–113. [PubMed: 16239926]

Sottile V, Seuwen K, Kneissel M. Enhanced marrow adipogenesis and bone resorption in estrogen-deprived rats treated with the PPARgamma agonist BRL49653 (rosiglitazone). Calcif Tissue Int. 2004; 75:329–337. [PubMed: 15549648]

Syed FA, Oursler MJ, Hefferanm TE, Peterson JM, Riggs BL, Khosla S. Effects of estrogen therapy on bone marrow adipocytes in postmenopausal osteoporotic women. Osteoporos Int. 2008; 19:1323–1330. [PubMed: 18274695]

Syed FA, Fraser DG, Monroe DG, Khosla S. Distinct effects of loss of classical estrogen receptor signaling versus complete deletion of estrogen receptor alpha on bone. Bone. 2011; 49:208–216. [PubMed: 21458604]

Walker VR, Korach KS. Estrogen receptor knockout mice as a model for endocrine research. ILAR J. 2004; 45:455–461. [PubMed: 15454684]

Wend K, Wend P, Krum SA. Tissue-specific effects of loss of estrogen during menopause and aging. Front Endocrinol. 2012; 3:19.

Zhao JW, Gao ZL, Mei H, Li YL, Wang Y. Differentiation of human mesenchymal stem cells: The potential mechanism for estrogen-induced preferential osteoblast versus adipocyte differentiation. Am J Med Sci. 2011; 341:460–468. [PubMed: 21289500]

Zimmermann R, Lass A, Haemmerle G, Zechner R. Fate of fat: The role of adipose triglyceride lipase in lipolysis. Biochim Biophys Acta. 2009; 1791:494–500. [PubMed: 19010445]

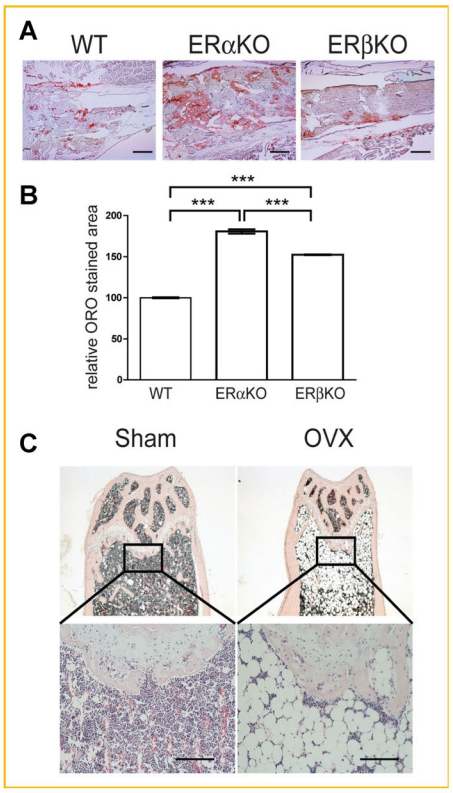


**Fig. 1.**

ERα deficiency increases bone marrow fat. A: Images of decalcified (for 3 days in Decal Stat) femur sections from 7-month-old WT, ERαKO, and ERβKO mice. Oil Red O was used to identify lipid droplets. Quantification is shown in (B) with three biological replicates. $^{***}P$ <0.001. C: Three-month-old wild-type mice were ovariectomized or sham operated. After two months the bone was fixed and femur sections were stained with H&E. Scale bar, 250 μm in A, 100 μm in C.

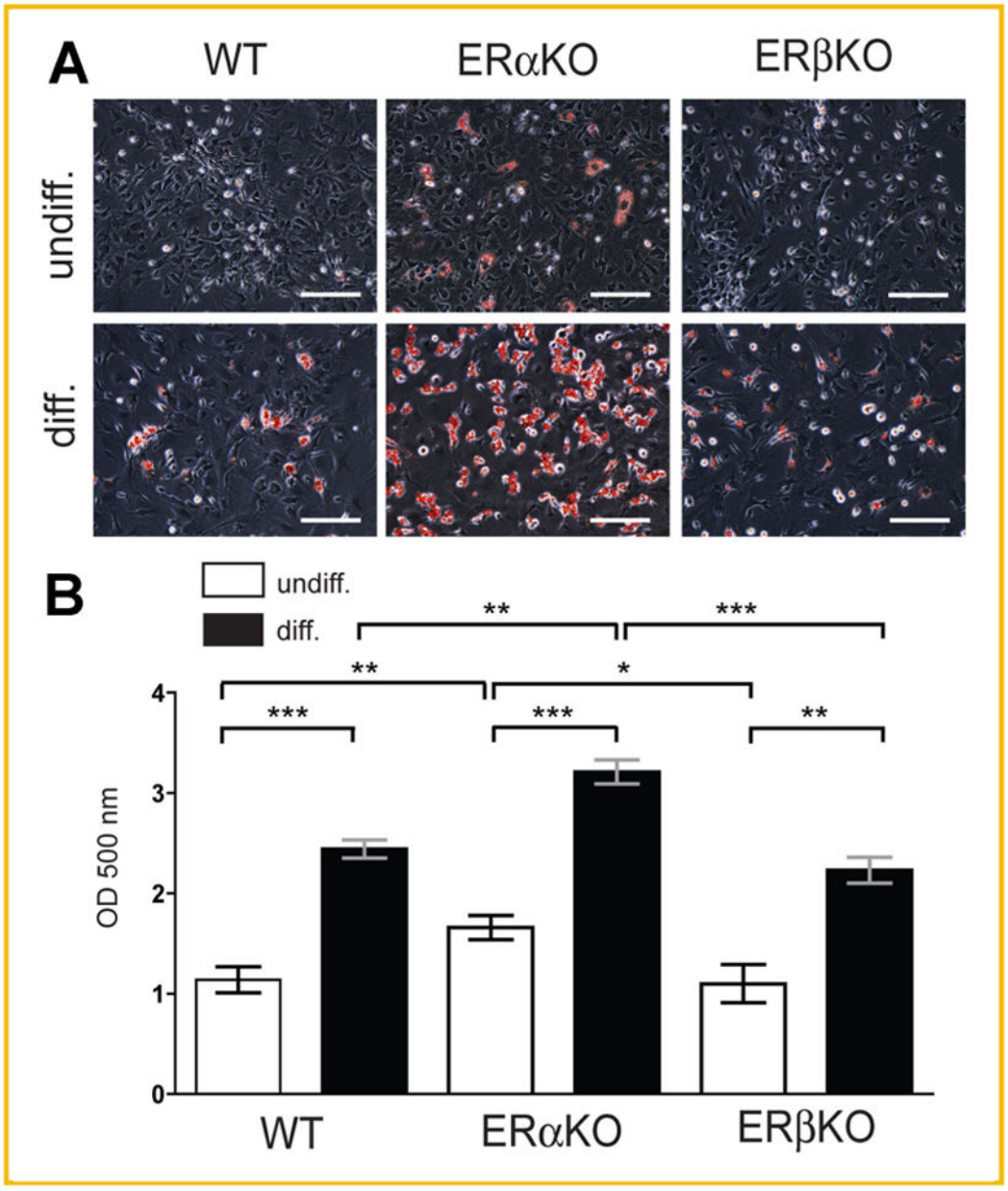


**Fig. 2.**

ERα inhibits adipogenesis in vitro. A: Colony forming unit adipocyte assay of bone marrow-derived mesenchymal stem cells from 4-month-old WT, ERαKO, and ERβKO mice. Oil Red O (ORO) stain was used to identify lipid droplets. Upper panel shows undifferentiated cells (undiff.) and lower panel depicts cells differentiated into adipocytes (diff.). B: Quantification from A is shown: ORO was eluted from triplicates and the OD was measured at 500 nm. $^{*}P<0.05$, $^{**}P<0.01$, $^{***}P<0.001$. Scale bar, 100 μm in A.

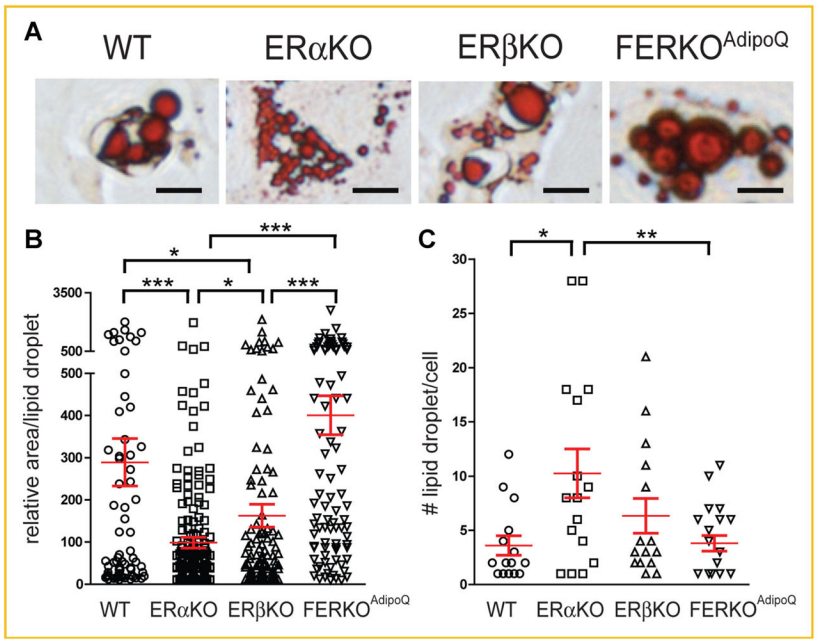


**Fig. 3.**

Absence of ERα decreases lipid droplet size. A: Representative images of bone marrow-derived mesenchymal stem cells differentiated into adipocytes from 4-month-old WT, ERαKO, ERβKO and 7-month-old FERKO$^{AdipoQ}$ mice. Oil Red O (ORO) stain was used to identify lipid droplets. B,C: Quantifications from A of the stained ORO lipid droplet size (relative area per lipid droplet) (B) and the number of lipid droplets per cell (C) are shown. Error bars represent mean ±SEM. $^{*}P<0.05$, $^{**}P<0.01$, $^{***}P<0.001$. Scale bar, 10 μm in A.

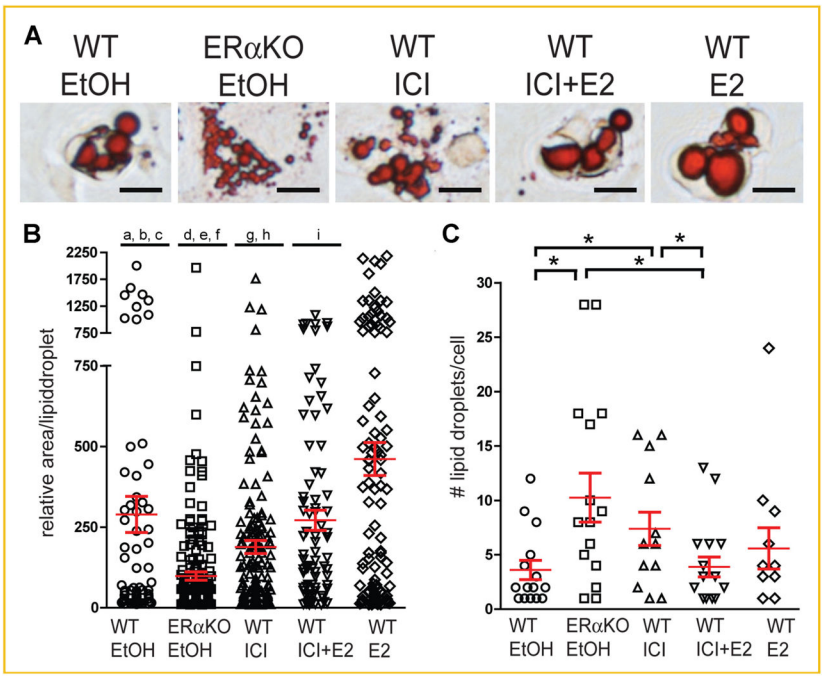


**Fig. 4.**

E2 signaling regulates lipid droplet size. A: Representative images of bone marrow-derived mesenchymal stem cells differentiated into adipocytes from 4-month-old WT and ERαKO mice. Cells from WT mice were treated with 10 nM ICI 182,780 (ICI), 10 nM E2, or 10 nM ICI 182,780+ 10 nM E2. Oil Red O (ORO) stain was used to identify lipid droplets. B,C: Quantifications from A of the stained ORO lipid droplet size (relative area per lipid droplet) (B) and the number of lipid droplets per cell (C) are shown. In B the following *P* values are depicted: $^{a}P<0.001$; Comparison between WT EtOH and ERαKO EtOH, $^{b}P<0.05$; Comparison between WT EtOH and WT 10 nM ICI 182,780, $^{c}P<0.05$; Comparison between WT EtOH and WT 10 nM E2, $^{d}P<0.001$; Comparison between ERαKO EtOH and WT 10 nM ICI 182,780, $^{e}P<0.001$; Comparison between ERαKO EtOH and WT 10 nM ICI 182,780+ 10 nM E2, $^{f}P<0.001$; Comparison between ERαKO EtOH and WT 10 nM E2, $^{g}P<0.05$; Comparison between WT 10 nM ICI 182,780 and WT 10 nM ICI 182,780+ 10 nM E2, $^{h}P<0.001$; Comparison between WT 10 nM ICI 182,780 and WT 10 nM E2, $^{i}P<0.01$; Comparison between WT 10 nM ICI 182,780 +10 nM E2 and WT 10 nM E2. Error bars represent mean ±SEM. $^{*}P<0.05$, $^{**}P<0.01$, $^{***}P<0.001$. Scale bar, 10 μm in A.

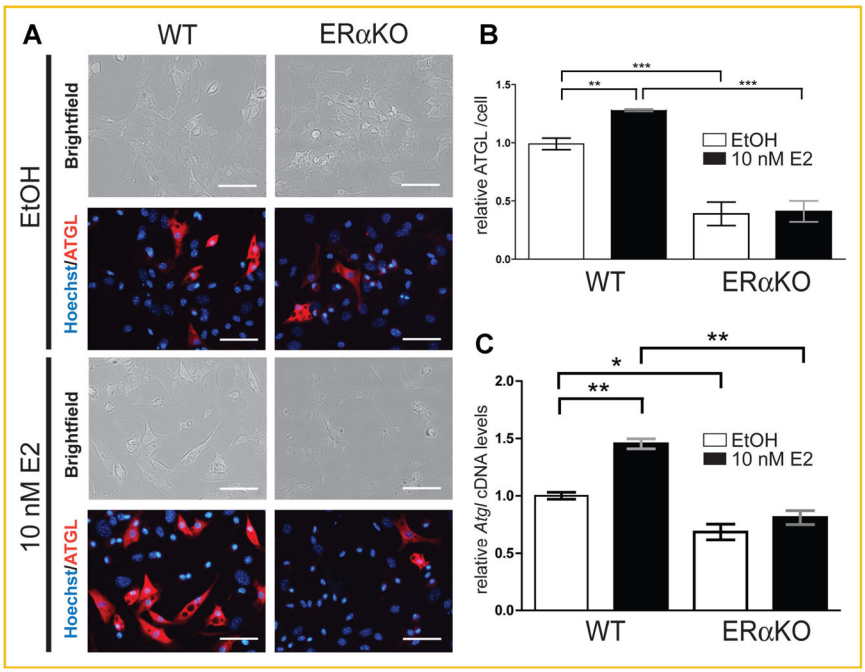


**Fig. 5.**

E2 regulates ATGL expression. A: Light and immunofluorescence microscopy (ATGL antibody stains ATGL protein in red, Hoechst stains nuclei in blue) of bone marrow-derived mesenchymal stem cells differentiated for 16 days into adipocytes from 4-month-old WT and ERαKO mice. The cells were treated for 16 days either with control (EtOH) or 10 nM E2. Quantification is shown in (B). C: Quantitative PCR of *Atgl* cDNA levels from bone marrow-derived mesenchymal stem cells differentiated into adipocytes for 16 days from 4-month-old WT and ERαKO mice. The cells were treated for 16 days either with control (EtOH) or 10 nM E2. RNA was obtained. Atgl mRNA was analyzed by qPCR and normalized to actin mRNA. $^{*}P<0.05$, $^{**}P<0.01$, $^{***}P<0.001$. Scale bar, 50 μm in A.

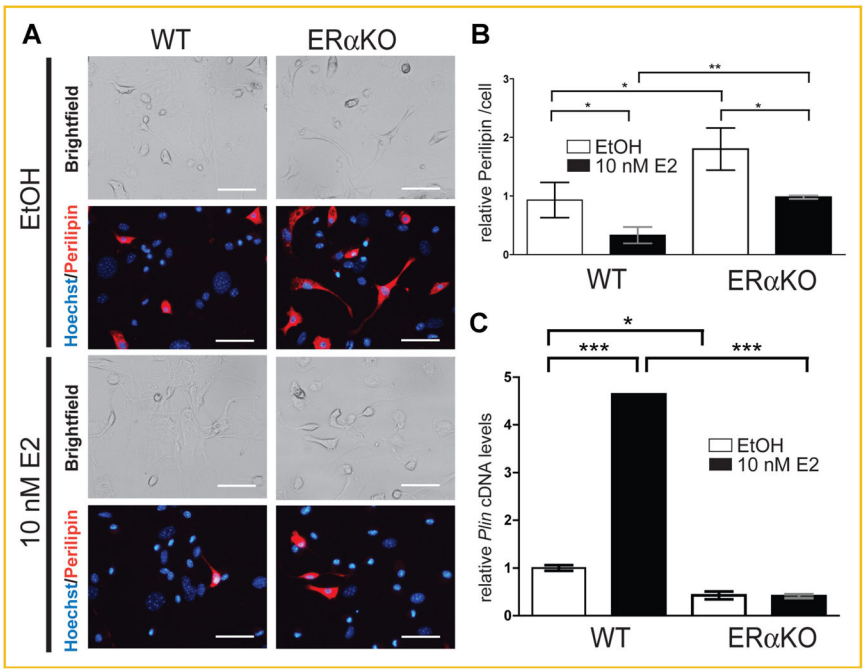


**Fig. 6.**

E2 regulates perilipin expression. A: Light and immunofluorescence microscopy (perilipin antibody stains perilipin protein in red, Hoechst stains nuclei in blue) of bone marrow-derived mesenchymal stem cells differentiated for 16 days into adipocytes from 4-month-old WT and ERαKO mice. The cells were treated for 16 days either with control (EtOH) or 10 nM E2. Quantification is shown in (B). C: Quantitative PCR of *Plin* cDNA levels of bone marrow-derived mesenchymal stem cells differentiated into adipocytes for 16 days from 4-month-old WT and ERαKO mice. The cells were treated for 16 days either with control (EtOH) or 10 nM E2. RNA was obtained. Plin mRNA was analyzed by qPCR and normalized to actin mRNA. $^{*}P<0.05$, $^{**}P<0.01$, $^{***}P<0.001$. Scale bar, 50 μm in A.